

# Fréchet Mean and $p$ -Mean on the Unit Circle: Decidability, Algorithm, and Applications to Clustering on the Flat Torus

Frédéric Cazals ✉

Université Côte d'Azur, France  
Inria, Sophia Antipolis, France

Bernard Delmas ✉

INRAe, Jouy-en-Josas, France

Timothee O'Donnell ✉

Université Côte d'Azur, France  
Inria, Sophia Antipolis, France

---

## Abstract

The center of mass of a point set lying on a manifold generalizes the celebrated Euclidean centroid, and is ubiquitous in statistical analysis in non Euclidean spaces. In this work, we give a complete characterization of the weighted  $p$ -mean of a finite set of angular values on  $S^1$ , based on a decomposition of  $S^1$  such that the functional of interest has at most one local minimum per cell. This characterization is used to show that the problem is decidable for rational angular values—a consequence of Lindemann's theorem on the transcendence of  $\pi$ , and to develop an effective algorithm parameterized by exact predicates. A robust implementation of this algorithm based on multi-precision interval arithmetic is also presented, and is shown to be effective for large values of  $n$  and  $p$ . We use it as building block to implement the k-means and k-means++ clustering algorithms on the flat torus, with applications to clustering protein molecular conformations. These algorithms are available in the Structural Bioinformatics Library (<http://sbl.inria.fr>).

Our derivations are of interest in two respects. First, efficient  $p$ -mean calculations are relevant to develop principal components analysis on the flat torus encoding angular spaces—a particularly important case to describe molecular conformations. Second, our two-stage strategy stresses the interest of combinatorial methods for  $p$ -means, also emphasizing the role of numerical issues.

**2012 ACM Subject Classification** Theory of computation → Computational geometry

**Keywords and phrases** Fréchet mean,  $p$ -mean, circular statistics, decidability, robustness, multi-precision, angular spaces, flat torus, clustering, molecular conformations

**Digital Object Identifier** 10.4230/LIPIcs.SEA.2021.15

**Supplementary Material** *Software*: <https://sbl.inria.fr/>

*Text (Documentation)*: [https://sbl.inria.fr/doc/Frechet\\_mean\\_S1-user-manual.html](https://sbl.inria.fr/doc/Frechet_mean_S1-user-manual.html)

**Acknowledgements** Chee Yap and Sylvain Pion are acknowledged for discussions on irrational number theory and number types, respectively.

## 1 Introduction

### 1.1 Statistics on manifolds and $p$ -means on $S^1$

**Fréchet mean and generalizations.** The celebrated center of mass of a point set  $P$  in a Euclidean space is the (a) point minimizing the sum of squared Euclidean distances to points in  $P$ . The center of mass plays a key role in data analysis at large, and in particular in principal components analysis since the data are centered prior to computing the covariance matrix and the principal directions. Generalizing these notions to non Euclidean spaces is an active area of research. Motivated by applications in structural biology (molecular conformations), robotics (robot conformations), and medicine (shape and relative positions



© Frédéric Cazals, Bernard Delmas, and Timothee O'Donnell;  
licensed under Creative Commons License CC-BY 4.0

19th International Symposium on Experimental Algorithms (SEA 2021).

Editors: David Coudert and Emanuele Natale; Article No. 15; pp. 15:1–15:16

Leibniz International Proceedings in Informatics



LIPICs Schloss Dagstuhl – Leibniz-Zentrum für Informatik, Dagstuhl Publishing, Germany

of organs), early work focused on direct generalizations of Euclidean notions. Analysis tailored to the unit circle and sphere were developed under the umbrella of directional statistics [2, 19, 20]. In a more abstract setting, generalizations of the center of mass in general metric spaces were first worked out – the so-called Fréchet mean [11], followed by a generalization to distributions on such spaces – the so-called Karcher mean [12, 3, 23].

In fact, previous works span two complementary directions. On the one hand, efforts have focused on mathematical properties of spaces generalizing affine spaces, so as to provide statistical summaries of ensembles in terms of geometric objects of small dimension. On the other hand, algorithmic developments have been performed proposed to compute such objects. The case of the unit circle  $S^1$  provides the simplest compact non Euclidean manifold to be analyzed. Despite its simplicity, this case turns out to be of high interest since  $S^1$  encodes angles, a particularly important case e.g. to describe molecular conformations. In the following, we focus on  $p$ -means defined on the unit circle  $S^1$ , for  $p > 1$ . (The case  $p = 1$  requires trivial adaptations.)

Consider  $n$  angles  $\Theta_0 = \{\theta_i\}_{i=1,\dots,n}$ . Practically, since real data are known with finite precision, we treat angles as rational numbers. Consider the embedding of an angle onto the unit circle, that is  $X(\theta) = (\cos \theta, \sin \theta)^T$ . The geodesic distance between two points  $X(\theta)$  and  $X(\theta_i)$  on  $S^1$ , denoted  $d(\cdot, \cdot)$ , satisfies

$$d(X(\theta), X(\theta_i)) = \min(|\theta - \theta_i|, 2\pi - |\theta - \theta_i|) = 2 \arcsin \frac{\|X(\theta) - X(\theta_i)\|}{2}. \quad (1)$$

Consider a set of positive weights  $\{w_i\}_{i=1,\dots,n}$ . For an integer  $p \geq 1$ , consider the function involving the weighted distances to all points, i.e.

$$F_p(\theta) = \sum_{i=1,\dots,n} w_i f_i(\theta), \text{ with } f_i(\theta) = d^p(X(\theta), X(\theta_i)). \quad (2)$$

We denote its minimum

$$\theta^* = \arg \min_{\theta \in [0, 2\pi)} F_p(\theta). \quad (3)$$

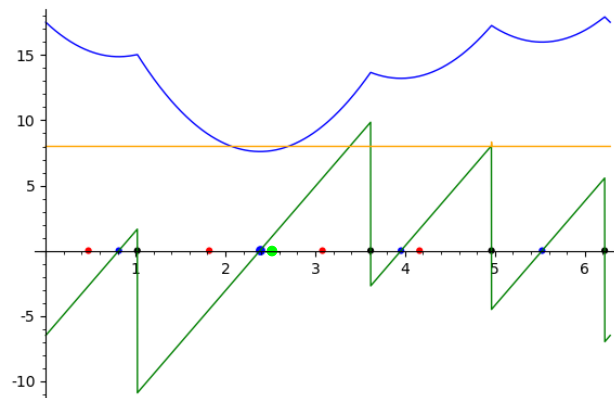
For units weights and  $p = 2$ , the value obtained is the Fréchet mean. In that case, the candidate minimizers (local minima of Eq. 2) form the vertices of a regular polygon [13]. The previous expression can also be seen as a distance to a point mass probability distribution on  $S^1$ . For a general probability distribution on  $S^1$ , necessary and sufficient conditions for the existence of a Fréchet mean have been worked out [9]. In the same paper, the authors propose a quadratic algorithm—regardless of numerical issues—to compute the Fréchet mean for the particular case of a point mass probability distribution. In a more general setting, a stochastic algorithm finding  $p$ -means wrt a general measure on the circle has also been proposed [4].

► **Remark 1.** In the subsequent sections, the weights in Eq. 2 are omitted – rational weights do not change our analysis. Our implementation, however, does use them.

**Robustness and numerical issues.** From a mathematical standpoint, computing the  $p$ -mean is a non-convex optimization problem, and one may assume that calculations are carried out in the standard real RAM computer model, which assumes that exact operations on real numbers are available at constant time per operation [24]. From a practical standpoint though, numbers in real computers are represented with finite precision [21]. The ensuing rounding errors are such that algorithms written in the real RAM model may loop, crash, or terminate with an erroneous answer, even for the simplest 2D geometric calculations [16].

Robust geometric algorithms, which deliver what they are designed for, can be developed using the Exact Geometric Computation (EGC) paradigm [27], which is central in the Computational Geometry Algorithms Library (CGAL) [1]. The EGC relies on so-called *exact predicates* and *constructions*. A predicate is a function whose output belongs to a finite set, while a construction exhibits a new geometric object from the input data. For example, the predicate `Sign`( $x$ ) returns the sign  $\{\text{negative}, \text{null}, \text{positive}\}$  of the arithmetic expression  $x$ . As we shall see, designing robust predicates for  $p$ -means on  $S^1$  is connected to transcendental number theory since expressions involving  $\pi$  are dealt with. In particular, one needs to evaluate the sign of such expressions, which raises decidability issues [8].

**Combinatorial complexity issues.** The computation of the  $p$ -means also raises a combinatorial complexity issue. Function  $F_p$  being a sum over  $n$  terms,  $k$  function evaluations yield a complexity  $O(kn)$ , which is quadratic if there is a linear number of local minima. Therefore, the fact that using candidate minimizers form a regular polygon [13] does not directly yield a linear time algorithm even if the angles are sorted. As we shall see, the piecewise maintenance of the expression of the function does so, though. For the sake of conciseness, combinatorial complexity is plainly referred to as complexity in the sequel.



■ **Figure 1** Fréchet mean of four points on  $S^1$ . (Functions) blue: function  $F_2$ ; green: derivative  $F'_2$ ; orange: second derivative  $F''_2$  (Points) red bullets: data points; black bullets: antipodal points; blue bullets: local minima of the function; large blue bullet: Fréchet mean  $\theta^*$ ; green bullet: circular mean Eq. 14.

## 1.2 Contributions

This paper makes three contributions regarding  $p$ -means of a finite point set. First, we show that the function  $F_p$  is determined by a very simple combinatorial structure, namely a partition of  $S^1$  into circle arcs. Second, we give an explicit expression for  $F_p$ , deduce that the problem is decidable, and present an algorithm computing  $p$ -means. Third, we present an effective and robust implementation, based on multi-precision interval arithmetic.

## 2 $p$ -mean of a finite point set on $S^1$ : characterization

### 2.1 Notations

In the following, angles are in  $[0, 2\pi)$ . We first define:

## 15:4 Fréchet Mean

► **Definition 2.** For each angle  $\theta_i \in [0, \pi)$ , we define  $\theta_i^+ = \theta_i + \pi$ . The set of all such angles is denoted  $\Theta^+ = \{\theta_i^+\}$ . For each angle  $\theta_i \in [\pi, 2\pi)$ , we define  $\theta_i^- = \theta_i - \pi$ . The set of all such angles is denoted  $\Theta^- = \{\theta_i^-\}$ . The antipodal set of  $\Theta_0$  is the set of angles  $\Theta^\pm = \Theta^+ \cup \Theta^-$ .

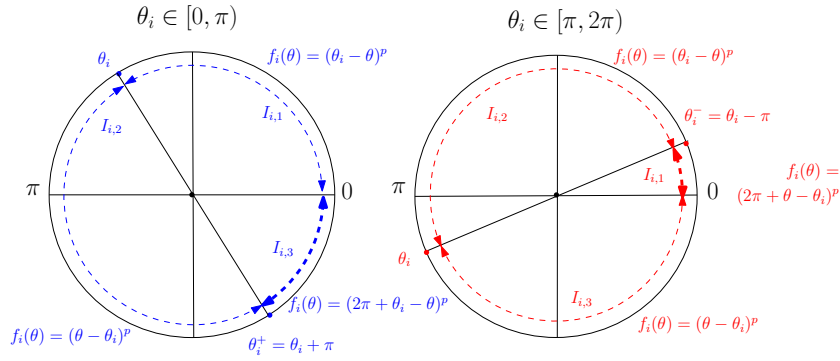
Altogether, these angles yield the larger set

$$\Theta = \Theta_0 \cup \Theta^\pm. \quad (4)$$

The  $2n$  angles in  $\Theta$  are generically denoted  $\alpha_i$  or  $\alpha_j$ . Note however that when referring to an angle in the continuous interval  $[0, 2\pi)$ ,  $\theta$  is used.

To each angle  $\theta_i$ , we associate three so-called *elementary intervals* (Fig. 2):

- $\theta_i \in [0, \pi) : I_{i,1} = (0, \theta_i), I_{i,2} = (\theta_i, \theta_i^+), I_{i,3} = (\theta_i^+, 2\pi)$ .
- $\theta_i \in [\pi, 2\pi) : I_{i,1} = (0, \theta_i^-), I_{i,2} = (\theta_i^-, \theta_i), I_{i,3} = (\theta_i, 2\pi)$ .



■ **Figure 2** The partition of  $S^1$  into circle arcs, and the piecewise functions defining  $F_p$ . The three elementary intervals defined by angles in  $[0, \pi)$  and  $[\pi, 2\pi)$  respectively. Bold circle arcs indicate that  $f_i$  has a transcendental expression i.e. involves  $\pi$ .

## 2.2 Partition of $S^1$

We also consider the partition of  $[0, 2\pi)$  induced by the intersection of the  $3n$  intervals  $\{I_{i,1}, I_{i,2}, I_{i,3}\}$  (Fig. 2). More specifically, we choose one interval (out of three) for each function  $f_i$ , and intersect them all:

► **Definition 3.** The elementary intervals  $I_{i,j}$  define a partition of  $S^1$  based on the following intervals:

$$\mathcal{I} = \left\{ \bigcap_{i=1, \dots, n} (I_{i,1} \vee I_{i,2} \vee I_{i,3}) \text{ with } \bigcap_{i=1, \dots, n} I_{i,\cdot} \neq \emptyset \right\}. \quad (5)$$

In the following, open intervals from  $\mathcal{I}$  are denoted  $(\alpha_j, \alpha_{j+1})$ .

► **Remark 4.** From the previous definition, it appears that the intervals in  $\mathcal{I}$  may be ascribed to nine types since the left endpoint is an angle  $\theta_i$  or an antipodal angle  $\theta_i^+$  or  $\theta_i^-$ , and likewise for the right endpoint.

### 2.3 Piecewise expression for $F_p$

We use the previous intervals to describe the piecewise structure of  $F_p$ . We define the following piecewise functions (Fig 2):

$$\theta_i \in [0, \pi) : f_i(\theta) = \begin{cases} (\theta_i - \theta)^p, & \text{for } \theta \in I_{i,1}, \\ (\theta - \theta_i)^p, & \text{for } \theta \in I_{i,2}, \\ (2\pi + \theta_i - \theta)^p, & \text{for } \theta \in I_{i,3}. \end{cases} \quad (6)$$

$$\theta_i \in [\pi, 2\pi) : f_i(\theta) = \begin{cases} (2\pi + \theta - \theta_i)^p, & \text{for } \theta \in I_{i,1}, \\ (\theta_i - \theta)^p, & \text{for } \theta \in I_{i,2}, \\ (\theta - \theta_i)^p, & \text{for } \theta \in I_{i,3}. \end{cases} \quad (7)$$

The previous equations give the piecewise expression of  $F_p(\theta)$  (Eq. 2), from which one derives the following, which characterizes the derivative at points in  $\alpha_j \in \Theta$ :

$$\Delta f'_{i|\theta} = \lim_{\theta \searrow \alpha_j} f'_i(\theta) - \lim_{\theta \nearrow \alpha_j} f'_i(\theta) \quad (8)$$

► **Remark 5.** Let  $\theta_{\max}$  be the antipodal value of the largest  $\theta_i \in \Theta_0$  larger than  $\pi$ , and  $\theta_{\min}$  the antipode of the smallest  $\theta_i \in \Theta_0$  smaller than  $\pi$ . The function  $F_p$  is transcendental in  $[0, \theta_{\max})$  and  $(\theta_{\min}, 2\pi]$  – its expression involves  $\pi$ . Also, the function  $F_p$  is algebraic on  $(\theta_{\max}, \theta_{\min})$ . See Fig. 2.

Using Eq. 8, the following is immediate:

► **Lemma 6.** For  $p > 1$ , the function  $f_i$  and its derivatives satisfy:

- The function  $f_i$  is continuous on  $S^1$ .
- The derivative  $f'_i$  is continuous on  $S^1$  except at the antipodal value of  $\theta_i$ , where  $\Delta f'_{i|\text{antipode}(\theta_i)} = -2p \pi^{p-1}$ .
- The second order derivative  $f''_i$  is non negative on  $S^1$ .

The previous lemma tells us that  $F'_p$  incurs drops at antipodal points, and then keeps increasing again on the interval starting at that point. Finding local minima of  $F_p$  therefore requires finding those intervals from  $\mathcal{I}$  where  $F'_p$  vanishes, which happens at most once:

► **Lemma 7.** For  $p > 1$ , the function  $F_p$  has at most one local min. on each interval in  $\mathcal{I}$ .

## 3 Algorithm

The observations above are not sufficient to obtain an efficient algorithm: since there are  $2n$  intervals and since the function has linear complexity on each of them, a linear number of function evaluations has quadratic complexity. We get around this difficulty by maintaining the expression of the function at angles in  $\Theta$ .

### 3.1 Analytical expressions and nullity of $F'_p$

**The function  $F_p$  and its derivative.** We first derive a compact, analytical expression of  $F_p$  and  $F'_p$ . Following Eqs. 6 and 7, the expressions of  $f_i(\theta)$  and  $f'_i(\theta)$  can be written as

$$f'_i(\theta) = k_i \times (a_i + \varepsilon_i \theta)^{p-1}, \text{ with } k_i \in \{-p, p\}, a_i \in \{-\theta_i, 2\pi - \theta_i, \theta_i, 2\pi + \theta_i\}, \varepsilon_i \in \{-1, +1\}. \quad (9)$$

## 15:6 Fréchet Mean

On open intervals  $(\alpha_j, \alpha_{j+1})$ , the function reads as the following polynomial

$$F_p(\theta) = \sum_{i=1}^n (a_i + \varepsilon_i \theta)^p = \sum_{j=0}^p b_j \theta^j, \quad \text{with } b_j = \sum_{i=1}^n \binom{p}{j} a_i^{p-j} \varepsilon_i^j. \quad (10)$$

Similarly, the derivative  $F'_p(\theta)$  reads as a degree  $p - 1$  polynomial:

$$F'_p(\theta) = \sum_{i=1}^n k_i (a_i + \varepsilon_i \theta)^{p-1} = \sum_{j=0}^{p-1} c_j \theta^j, \quad \text{with } c_j = \sum_{i=1}^n k_i \binom{p-1}{j} a_i^{p-1-j} \varepsilon_i^j. \quad (11)$$

In the following, we assume that the coefficients of  $F_p$  and  $F'_p$  are stored in two vectors  $B$  and  $C$  of size  $p + 1$  and  $p$  respectively, so that evaluating the function or its derivative at a given  $\theta$  has cost  $O(p)$ .

**Nullity of  $F'_p$ : algebraic versus transcendental expressions.** The previous equations call for two important comments. First, from the combinatorial complexity standpoint, if the coefficients of the polynomials are known, evaluating  $F_p$  and  $F'_p$  has cost  $O(p)$ . Second, from the numerical standpoint, locating local minima of  $F_p$  requires finding intervals from  $\mathcal{I}$  on which  $F'_p$  vanishes. Identifying such intervals is key to the robustness of our algorithm. Practically, since an interval is defined by two consecutive values in the set  $\Theta$ , we need to check that the sign of  $F'_p$  differs at these endpoints. The cornerstone is therefore to decide the sign of  $F'_p$  at angles in  $\Theta$  (input angles or their antipodes), and the following is a simple consequence of Lindemann's theorem on the transcendence of  $\pi$ :

► **Lemma 8.** *If the angular values  $\theta_i \in \Theta_0$  are rational numbers, checking whether  $F'_p(\alpha_i) \neq 0$  for any  $\alpha_i \in \Theta$  is decidable. Moreover, when  $F'_p$  has a transcendental expression and  $\alpha_i$  is rational,  $F'_p \neq 0$ .*

**Proof.** We first consider the case  $\alpha_i \in \Theta_0$ , and distinguish the two types of intervals – see Remark 5. First, consider an interval where  $F_p$  has an algebraic expression. We face a purely algebraic problem, and deciding whether  $F'_p(\alpha_i) \neq 0$  can be done using classical bounds, e.g. Mahler bounds [18, 28]. Second, consider an interval where  $F_p$  has a transcendental expression. Then,  $F'_p(\alpha_i)$  can be rewritten as a polynomial of degree  $p - 1$  in  $\pi$ . Lindemann's theorem on the transcendence of  $\pi$  implies that  $F'_p(\alpha_i) \neq 0$ .

Consider now the case where  $\alpha_i \in \Theta^\pm$ , that is  $\alpha_i = \alpha_j \pm \pi$ . Each individual term  $f'_i(\alpha_i)$  also has the form  $(c_i \pi + q_i)^{p-1}$ , with  $c_i \in \mathbb{N}$  and  $q_i \in \mathbb{Q}$ , so that the latter case also applies. ◀

### 3.2 Algorithm

Upon creating and sorting the set  $\Theta$ , which has complexity  $O(n \log n)$ , the algorithm involves four steps for each interval in  $\mathcal{I}$ .

**Identify the intervals where  $F'_p$  vanishes.** By lemmas 6 and 7, there is at most one local minimum per interval, which requires checking the signs of  $F'_p$  to the right and left bounds of an interval  $(\alpha_j, \alpha_{j+1})$ . Using the functional forms encoded in vector  $C$ , computing these derivatives has the same complexity as the previous step. However, this step calls for two important comments:

- For  $\alpha_i \in \Theta$ , checking whether  $F'_p(\alpha_i) \neq 0$  is decidable – Lemma 8. However, the arithmetic nature of the number  $\alpha_i$  must be taken into account, as rational numbers (input angles) and transcendental numbers (antipodal points) must be dealt with using different arithmetic techniques. See below.
- Not all intervals  $(\alpha_j, \alpha_{j+1})$  can provide a root. Indeed, once  $F'_p(\alpha_i) > 0$ , since the individual second order derivatives are positive,  $F'_p$  cannot vanish until one crosses one  $\alpha_j \in \Theta^\pm$ . As we shall see, this observation is easily accommodated in Algorithm 1.

In the following, we denote  $SD(p-1)$  the cost of deciding the sign (negative, zero, positive) of  $F'_p(\theta)$ , for  $\theta \in \Theta$ .

**Compute the unique root of  $F'_p$ .** Since  $F'_p$  is piecewise polynomial, finding its real root has constant time complexity for  $p \leq 5$ . Otherwise, a numerical method can be used [17]. In the following, we denote  $RF(p-1)$  the cost of isolating the real root of a degree  $p-1$  polynomial.

**Evaluate  $F_p$  at a local minimum.** Once the angle  $\theta_m$  corresponding to a local minimum has been computed, we evaluate  $F_p(\theta_m)$  using Eq. 10. This evaluation has  $O(p)$  complexity since the coefficients of the polynomial are known.

**Maintain the polynomials  $F_p$  and  $F'_p$ .** Following Eqs. 10 and 11, the function and its derivative only change when crossing an angle from  $\Theta$ . At such an angle, updating the vectors  $B$  and  $C$  has complexity  $O(p)$ . Overall, this step therefore has complexity  $O(np)$ .

We summarize with the following output-sensitive complexity:

- ▶ **Theorem 9.** *Algorithm 1 computes the  $p$ -mean with  $O(n \log n + np + nSD(p-1) + kRF(p-1) + kp)$  complexity, with  $k$  the number of local minima of  $F_p$ .*

### 3.3 Generic implementation

In the following, we present an implementation of our algorithm based on predicates, i.e. functions deciding branching points.

**Pseudo-code, predicates and constructions.** Our algorithm (Algo. 1) takes as input a list of angular values (in degrees or radians) and the value of  $p$ . Following Remark 1, an optional file containing the weights may be passed. If  $p > 5$ , we take for granted an algorithm computing the root of  $F'_p$  on an interval. As a default, we resort to a bisection method which divides the interval into two, checks which side contains the unique root of  $F'_p$ , and iterates until the width of the interval is less than some user specified value  $\tau$  (supporting information (SI) Algo. 3). The interval returned is called the *root isolation interval*. Our algorithm was implemented in generic C++ in the Structural Bioinformatics Library [6], as a template class whose main parameter is a geometric kernel providing the required predicates and constructions. We now discuss these—see Sec. 3.4 for their robust implementation.

**Predicates.** The algorithm involves two predicates:

- **Sign( $F'_p(\theta)$ ).** Predicate used to determine the sign of the  $F'_p(\theta)$  with  $\theta \in [0, 2\pi)$  (SI Algo. 3).
- **Interval\_too\_wide( $\theta_l, \theta_r$ ).** Predicate used to determine whether the root isolation interval has width less than  $\tau$  (SI Algo. 3). It is true if  $\theta_r - \theta_l > \tau$ , and false otherwise.

**Constructions.**

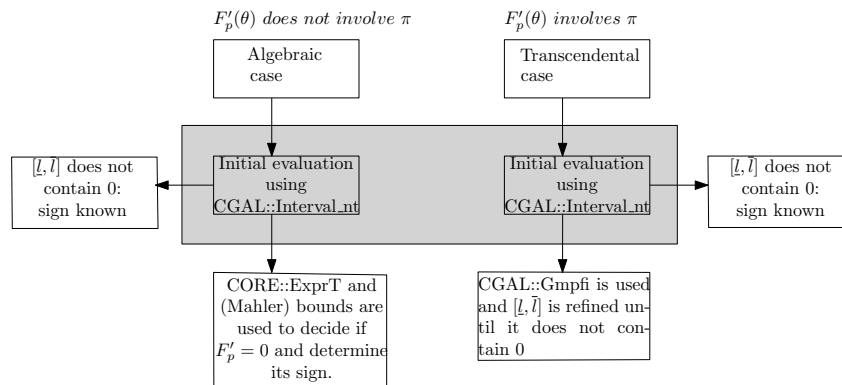
- **Updating representations.** Updating the coefficients in  $B$  and  $C$  is necessary at each  $\alpha_i \in \Theta$ : for  $F_p(\theta)$  (resp.  $F'_p(\theta)$ ), we subtract the contribution of  $f_i(\theta)$  (resp.  $f'_i(\theta)$ ) before  $\alpha_i$ , and add that of  $f_i(\theta)$  (resp.  $f'_i(\theta)$ ) after  $\alpha_i$ .
- **Find\_root.** To computing the root of  $F'_p$  on an interval  $(\alpha_j, \alpha_{j+1})$ , we resort to a bisection method  $p > 3$  (SI Algo. 3), with radical based formulae otherwise.

► **Remark 10.** A kernel based on floating point number types, the `double` type in our case, is easily assembled, see `SBL::GT::Inexact_predicates_kernel_for_frechet_mean` in SI Sec. 3.5. As noticed earlier, it comes with no guarantee. In particular, the algorithm may terminate with an erroneous result if selected predicates are falsely evaluated.

### 3.4 Robust implementation based on exact predicates

**Number types for lazy evaluations.** Following the Exact Geometric Computation exact predicates are gathered in a *kernel*. We circumvent rounding errors using interval number types which are certified to contain the exact value of interest. That is, an expression  $x$  is represented by the interval  $[\underline{x}, \bar{x}] \ni x$ . The bounds of these intervals may have a fixed precision, which corresponds to the `CGAL::Interval_nt` number type [1]. Or the bounds may be multiprecision, e.g. `Gmpfr` from `Mpfr` [10], which corresponds to the `CGAL::Gmpfi` type [1]. We now explain how these types are used to code exact predicates.

**The Sign predicate.** We distinguish the algebraic and transcendental cases, performing multiprecision calculations only if needed (Fig. 3).



■ **Figure 3** Number types used in the `Sign` predicate. Note that `CGAL::Interval_nt` is used in the algebraic and transcendental cases, while the remaining number types are only used if required.

- **Transcendental case: multiprecision interval arithmetic.** When  $F_p$  is transcendental and  $\alpha_i$  rational,  $F'_p(\alpha_i)$  is positive or negative (lemma 8). Another case where  $F'_p(\alpha_i) \neq 0$  is when  $\alpha_i \in \Theta^\pm$ . In our implementation this situation is faced in two cases. First, in the main algorithm (Algo. 1), `Sign(l)` or `Sign(r)`:  $l$  and  $r$  are transcendental if  $\alpha_i \in \Theta^\pm$ . Second, in the root finding algorithm (SI Algo. 3), `Sign(F'_p(c))`:  $c$  is transcendental if  $\alpha_{i-1}$  or  $\alpha_i \in \Theta^\pm$ . In both cases, we proceed in a lazy way: first, we try to conclude using `CGAL::Interval_nt`; if this interval contains zero, we switch to `CGAL::Gmpfi` (Fig. 3), refine the interval bounds, and conclude. Refining the interval consists of iteratively doubling the number of bits used to describe all numbers—including  $\pi$ , until a conclusion can be reached.



■ **Algorithm 1**  $p$ -mean calculation: generic algorithm for  $p > 1$  in the real RAM model.

---

```

1:  $\Theta$ : vector[1, 2n] containing all the angles
2: B: vector[1, p + 1] to store the coefficients of the polynomial  $F_p(\theta)$  Eq. 10
3: C: vector[1, p] to store the coefficients of the polynomial  $F'_p(\theta)$  Eq. 11
4:  $\theta^*$  // Angle corresponding to the global minimum of  $F_p$ 
5: Root_remains = true // flag indicating whether a root must be sought on  $(\alpha_j, \alpha_{j+1})$ 
6:
7: // Initialization
8: Compute  $\Theta^\pm$  and form sorted  $\Theta$ 
9:  $\alpha_0$ : first angle in  $\Theta$ 
10: Store the coefficients of  $F_p$  into the vector B for the interval  $(0, \alpha_0)$ 
11: Store the coefficients of  $F'_p$  into vector C for the interval  $(0, \alpha_0)$ 
12: Compute  $l \leftarrow F'_p(\theta)$  for  $\theta \rightarrow 0^+$  using Eq. 11 and vector C
13: Update_root(Sign( $l$ ))//Updates Root_remains see SI Algo. 2
14: if Sign( $l$ ) is null then
15:   Compute  $F_p(0)$  using vector B and Eq. 10, and possibly update  $\theta^*$ .
16:
17: // For each angle, handle {interval ending, coefficients in B and C, interval starting}
18: for all  $\alpha_i$  in  $\Theta$  do
19:   if Root_remains then
20:     Compute  $r \leftarrow F'_p(\theta)$  for  $\theta \rightarrow \alpha_i^-$  using Eq. 11 and vector C
21:     Update_root(Sign( $r$ ))//Updates Root_remains see Algo. SI 2
22:     if Sign( $r$ ) is positive then
23:        $\theta_c \leftarrow$  Find_root( $\alpha_{i-1}, \alpha_i$ )
24:       Compute  $F_p(\theta_c)$  using vector B and Eq. 10, and possibly update  $\theta^*$ .
25:     else if Sign( $r$ ) is null then
26:       Compute  $F_p(\alpha_i)$  using vector B and Eq. 10, and possibly update  $\theta^*$ .
27:     Update the coefficients of  $F_p$  stored in vector B upon crossing  $\alpha_i$ 
28:     Update the coefficients of  $F'_p$  stored in vector C upon crossing  $\alpha_i$ 
29:     if  $\alpha_i \in \Theta^\pm$  then
30:       Compute  $l \leftarrow F'_p(\theta)$  for  $\theta \rightarrow \alpha_i^+$  using Eq. 11 and vector C
31:       Update_root(Sign( $l$ ))//Updates Root_remains see SI Algo. 2
32:       if Sign( $l$ ) is null then
33:         Compute  $F_p(\alpha_i)$  using vector B and Eq. 10, and possibly update  $\theta^*$ .
34:
35: // Process the interval ending at  $2\pi$ 
36: Compute  $r \leftarrow F'_p(\theta)$  for  $\theta \rightarrow 2\pi^-$  using Eq. 11 and vector C
37: if Root_remains then
38:   if Sign( $r$ ) is positive then
39:      $\theta_c \leftarrow$  Find_root( $\theta_{2n}, 2\pi$ )
40:     Compute  $F_p(\theta_c)$  using vector B and Eq. 10, and possibly update  $\theta^*$ 
41:   else if Sign( $r$ ) is null then
42:     Compute  $F_p(2\pi)$  using vector B and Eq. 10, and possibly update  $\theta^*$ .

```

---

• **Algebraic case: zero separation bounds.** When  $F_p$  has a rational expression and  $\alpha_i$  is rational,  $\text{Sign}(F_p'(\alpha_i))$  may be zero (SI Fig. 7). In this case, an input angle may also correspond to a local minimum of  $F_p$ . To decide whether  $F_p'(\alpha_i) = 0$ , we resort to zero separation bounds and multiprecision interval arithmetic.

Let us consider  $F_p'(\alpha_i)$  as an arithmetic expression  $E$ , using a number of authorized operations ( $\pm, \times, /$  in our case). A separation bound is a function  $\text{sep}$  such that the value  $\xi$  of expression  $E$  is lower bounded by  $\text{sep}(E)$  in the following manner:

$$\text{If } \xi \neq 0 \text{ then } \text{sep}(E) \leq |\xi| \quad (12)$$

Considering  $\tilde{\xi}$  an approximation of  $\xi$  and  $\Delta$  an upper bounded error  $|\tilde{\xi} - \xi|$ .

$$\text{If } |\tilde{\xi}| + \Delta < \text{sep}(E) \text{ then } \xi = 0. \quad (13)$$

Practically, we proceed in a lazy way, in two steps (Fig. 3). First, using `CGAL::Interval_nt` with double precision, we check whether we can conclude on  $F_p'(\alpha_i) \neq 0$ . If not—the interval contains zero, we use `CORE::ExprT[15]` to determine the zero separation bound and decide if  $F_p'(\alpha_i) = 0$ . If not, we finally determine the sign.

**Predicate `Interval_too_wide`**( $\theta_l, \theta_r$ ). Returns true when  $\underline{\theta}_r - \overline{\theta}_l > \tau$ , false if  $\overline{\theta}_r - \underline{\theta}_l \leq \tau$ . Similarly to the sign predicate, we distinguish the transcendental and algebraic cases to check whether  $\theta_l - \theta_r - \tau = 0$ . Supposing  $\tau$  and  $\Theta_0$  are rational  $\theta_l - \theta_r - \tau$  is transcendental if the initial  $\alpha_{i-1}$  or  $\alpha_i \in \Theta^\pm$ . If transcendental the interval is refined in the same way as the transcendental case of the `Sign` predicate. Otherwise the expression is algebraic and the precision is raised until an exact computation can be performed.

### 3.5 Software availability

The source code is available in the package *Frechet mean for  $S^1$*  of the Structural Bioinformatics Library (SBL), a library proposing state-of-the art methods in computational structural biology [6], see [https://sbl.inria.fr/doc/Frechet\\_mean\\_S1-user-manual.html](https://sbl.inria.fr/doc/Frechet_mean_S1-user-manual.html) and <https://sbl.inria.fr/>.

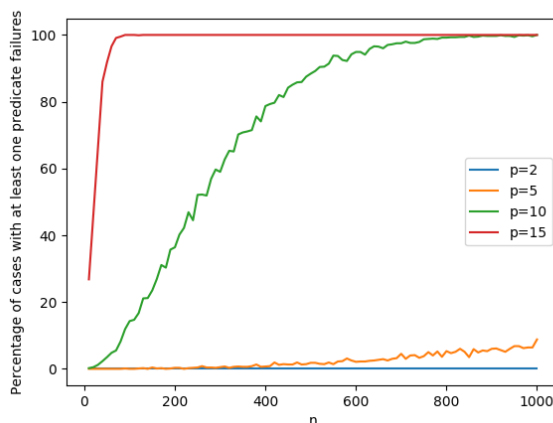
For end-users, the package provides executables corresponding to the robust and non-robust implementations. Given a list of angles and the value of  $p$ , the program returns sorted list of pairs (angular value of local minimum, function value) by increasing value of  $F_p$ . A Jupyter notebook `Frechet_mean_S1.ipynb` using SAGE (<https://www.sagemath.org/>) is also provided.

For developers, The C++ code of our algorithm is provided in the class `SBL::GT::Frechet_mean_S1`, which is templated by the kernel. Two kernels are provided, namely (i) Non-robust kernel: `SBL::GT::Inexact_predicates_kernel_for_frechet_mean`. A plain floating point(double) number type is used, and (ii) Robust kernel: `SBL::GT::Lazy_exact_predicates_kernel_for_frechet_mean`. See Sec. 3.4.

## 4 Experiments

### 4.1 Overview

Our experiments target three aspects, namely (i) robustness, (ii), comparison of the Fréchet mean against the classical circular mean, and (iii) computational complexity. Practically, three sets of angles are used. (Dataset 1) Randomly generated angles. (Dataset 2) So-called



■ **Figure 4** Fraction of program runs for which at least one predicate execution triggers refinement, as a function of  $n$  and  $p$ . The number of repeats for each value of  $n$  is 1000.

dihedral angles  $\chi_i$  in proteins, defined by 4 consecutive atoms on the side chains of amino acids. (Recall that a protein is a polymer of amino acids, and that the 20 natural a.a. differ by their so-called side chains. See Fig. 6 for an example.) These angles are known to be dependent, and correlations between them are key to reduce the dimensionality of the conformation space of proteins [26]. Using the Protein Data Bank, we retained 27093 PDB files with a resolution of 3 angstroms or better. For all polypeptide chains in these files, we computed all dihedral angles of all standard (20) amino-acids. This results in 240 classes of dihedral angles, containing from 50,227 to 439,793 observations. (Dataset 3) Also protein dihedral angles, but from a so-called *rotamer* library [25]. Rotamers (rotational isomers) are preferred conformations adopted by side chains, used to characterize protein conformations.

Note that in all cases, angles being given with finite precision (they are derived from experimentally determined atomic coordinates), they are treated as rational numbers.

## 4.2 Robustness

Using our robust interval-based implementation, we count the fraction of cases for which at least one predicate triggers refinement during an execution. We use sets of  $n \in [10, 1000]$  angles generated uniformly at random in  $[0, 2\pi)$ , and perform 1000 repeats for each value of  $n$  (SI Fig. 4). For large values of  $p$ , whenever  $n > 1000$ , all executions require interval refinement. Even for  $p = 2$  and  $n = 10^5$ , refinement is triggered in 1.3% of the cases. In all the cases where refinement was triggered, doubling the precision was sufficient to solve the predicate.

## 4.3 Fréchet mean

**Fréchet mean versus circular mean.** A classical way to estimate the circular mean of a set of angles is the *resultant* or *circular mean*, defined as follows [20]:

$$\bar{\theta} = \text{atan2}\left(\sum_i \sin \theta_i/n, \sum_i \cos \theta_i/n\right). \quad (14)$$

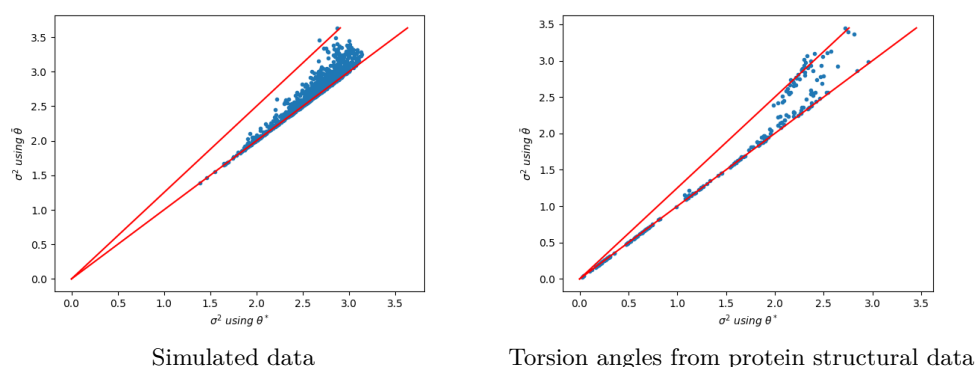
## 15:12 Fréchet Mean

The circular mean does not minimize  $F_p$ , but minimizes instead [14, Section 1.3]:

$$\bar{\theta} = \arg \min \sum_{i=1, \dots, n} d(\theta_i, \theta), \text{ with } d(\alpha, \beta) = 1 - \cos(\alpha - \beta). \quad (15)$$

Given a set of angles, we compare the variance of these angles with respect to the Fréchet mean  $\theta^*$  and the circular mean  $\bar{\theta}$ , respectively. Two datasets were used for such experiments: first, randomly generated sets of  $n = 30$  angles uniformly at random in  $[0, 2\pi)$ , with 1000 repeats; second, the aforementioned dihedral angles in protein structures.

For both types of data, the variance obtained for  $\bar{\theta}$  is significantly larger than that obtained for  $\theta^*$ , typically up to 25% (Fig. 5). This shows the interest of using  $\theta^*$  in data analysis in general, and to center angles prior to principal components analysis in particular.



■ **Figure 5** Variance of angles with respect to the Fréchet mean  $\theta^*$  and the circular average  $\bar{\theta}$ . (Left) Comparison using a simulated set with  $n = 30$  angles at random in  $[0, 2\pi)$ , with 1000 repeats. (Right) Comparison for the 243 classes dihedral angles in protein structures—see text. (Both panels) In red  $y = x$  and  $y = 5/4x$ .

### 4.4 Computation time and complexity

The complexity of Algorithm 1 (Theorem. 9) has three main components: the sorting step, the updates of vectors  $B$  and  $C$ , and the numerics. We wish in particular to determine whether the  $n \log n$  sorting term dominates.

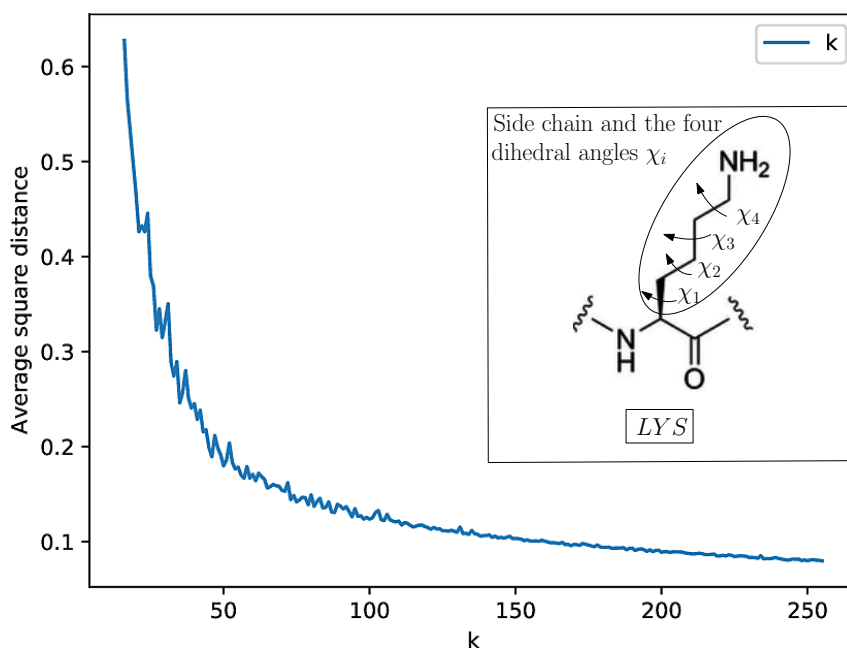
For  $p \in \{2, 5, 10, 15\}$ , we use sets of  $n \in [10^3, 10^5]$  angles generated uniformly at random in  $[0, 2\pi)$ , and perform 5 repeats for each value of  $n$ . For  $p = 2$ , the number of angles is pushed up to  $n = 10^7$ , with the same number of repeats. In any case, a linear complexity is practically observed (SI Fig. 8) showing that for the values of  $n$  used, the constants associated with the linear time update of the data structures and the numerics take over the  $n \log n$  term of the sorting step.

### 4.5 Application to clustering on the flat torus

Rotamers characterize the geometry of protein side chains (Sec. 4.1). State of the art rotameric libraries treat the dihedral angles independently [25]. For the a.a. lysine (LYS), (Fig. 6(Inset)), four angles and 3 canonical values for each yield  $3^4 = 81$  rotamers.

We undertake the problem of clustering side chains conformations using k-means++ [5]. While k-means is a classical clustering method, the problem solved is non convex and inferring the *right* number of clusters is always problematic [7]. One way to mitigate this

difficulty consists of tracking an elbow in the plot of the k-means functional [22]. Using the lysine (LYS) a.a. as example, we work directly on the 4D flat torus  $(S^1)^4$ , and center the data within a cluster using our Fréchet algorithm. Varying the value of  $k$  shows a sharp decline of the k-means++ criterion circa  $k = 40$ , and then a gradual straightening of the average squared distance (Fig. 6). Working directly on the flat torus therefore makes it possible to capture correlations between individual dihedral angles. The application to a significant reduction (factor of two or so) of rotamers will be reported elsewhere.



■ **Figure 6** k-means++ using Fréchet mean as center performed on 4-dimensional flat torus coding the conformational space of the side chain of the Lysine amino acid.  $x$ -axis: number of clusters  $k$ .  $y$ -axis: average squared distance to the closest cluster center.

## 5 Outlook

The Fréchet mean and the  $p$ -mean are of central importance as zero dimensional statistical summaries of data which do not live in Euclidean spaces. For the particular case of  $S^1$ , this paper develops the first robust algorithm computing the  $p$ -mean. Our algorithm is effective for large number of angular values and large values of  $p$  as well, yet, robustness requires predicates and constructions using interval multiprecision arithmetic. For the particular case of the Fréchet mean ( $p = 2$ ), we show that the circular mean should not be used for a substitute to the circular center of mass, as it results in a significantly larger variance.

We foresee two main developments. Application-wise, our results on protein side chain conformations hint at a significant reduction (factor of two or so) of rotamers, which should prove instrumental to foster the diversity of conformational explorations. Also, our centering procedure will help generalizing principal components analysis (PCA) on the flat torus. In theoretical realm, our strategy may be used both to study the intrinsic difficulty of computing  $p$ -means (in terms of lower bounds), and to design effective algorithms. Indeed, as evidenced by the  $S^1$  case, the combinatorial structure defined by the cut-loci of the points determines all key properties. A first case would be that of  $p$ -means on the unit sphere, for which there exist efficient algorithms to maintain arrangements of circles.

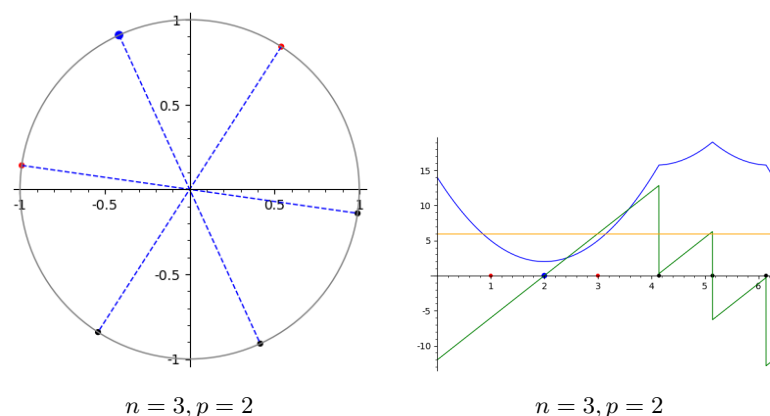
## References

- 1 CGAL, Computational Geometry Algorithms Library. <http://www.cgal.org>.
- 2 F. Allen and O. Johnson. Automated conformational analysis from crystallographic data. 4. statistical descriptors for a distribution of torsion angles. *Acta Crystallographica Section B: Structural Science*, 47(1):62–67, 1991.
- 3 M. Arnaudon and L. Miclo. Means in complete manifolds: uniqueness and approximation. *ESAIM: Probability and Statistics*, 18:185–206, 2014.
- 4 M. Arnaudon and L. Miclo. A stochastic algorithm finding  $p$ -means on the circle. *Bernoulli*, 22(4):2237–2300, 2016.
- 5 D. Arthur and S. Vassilvitskii.  $k$ -means++: The advantages of careful seeding. In *ACM-SODA*, page 1035. Society for Industrial and Applied Mathematics, 2007.
- 6 F. Cazals and T. Dreyfus. The Structural Bioinformatics Library: modeling in biomolecular science and beyond. *Bioinformatics*, 7(33):1–8, 2017. doi:10.1093/bioinformatics/btw752.
- 7 F. Cazals, D. Mazauric, R. Tetley, and R. Watrigant. Comparing two clusterings using matchings between clusters of clusters. *ACM J. of Experimental Algorithms*, 24(1):1–42, 2019. doi:10.1145/3345951.
- 8 E-C. Chang, S.W. Choi, D.Y. Kwon, H. Park, and C. Yap. Shortest path amidst disc obstacles is computable. *International Journal of Computational Geometry Applications*, 16(05n06):567–590, 2006.
- 9 B. Charlier. Necessary and sufficient condition for the existence of a Fréchet mean on the circle. *ESAIM: Probability and Statistics*, 17:635–649, 2013.
- 10 L. Fousse, G. Hanrot, V. Lefèvre, P. Pélissier, and P. Zimmermann. MPFR: A multiple-precision binary floating-point library with correct rounding. *ACM Transactions on Mathematical Software (TOMS)*, 33(2):13, 2007.
- 11 M. Fréchet. Les éléments aléatoires de nature quelconque dans un espace distancié. *Annales de l'institut Henri Poincaré*, 10(4):215–310, 1948.
- 12 K. Grove and H. Karcher. How to conjugate  $1$ -close group actions. *Mathematische Zeitschrift*, 132(1):11–20, 1973.
- 13 T. Hotz and s. Huckemann. Intrinsic means on the circle: Uniqueness, locus and asymptotics. *Annals of the Institute of Statistical Mathematics*, 67(1):177–193, 2015.
- 14 S.R. Jammalamadaka and A. SenGupta. *Topics in Circular Statistics*. World Scientific, 2001.
- 15 V. Karamcheti, C. Li, I. Pechtchanski, and C. Yap. A core library for robust numeric and geometric computation. In *Proceedings of the fifteenth annual symposium on Computational geometry*, pages 351–359. ACM, 1999.
- 16 L. Kettner, K. Mehlhorn, S. Pion, S. Schirra, and C. Yap. Classroom examples of robustness problems in geometric computations. *Computational Geometry*, 40(1):61–78, 2008.
- 17 A. Kobel, F. Rouillier, and M. Sagraloff. Computing real roots of real polynomials... and now for real! In *Proceedings of the ACM on International Symposium on Symbolic and Algebraic Computation*, pages 303–310. ACM, 2016.
- 18 C. Li, S. Pion, and C. Yap. Recent progress in exact geometric computation. *The Journal of Logic and Algebraic Programming*, 64(1):85–111, 2005.
- 19 M. MacArthur and J. Thornton. Conformational analysis of protein structures derived from nmr data. *Proteins: Structure, Function, and Bioinformatics*, 17(3):232–251, 1993.
- 20 K. Mardia and P. Jupp. *Directional statistics*, volume 494. John Wiley and Sons, 2009.
- 21 J.-M. Muller, N. Brunie, F. de Dinechin, C. Jeannerod, M. Joldes, V. Lefèvre, G. Melquiond, N. Revol, and S. Torres. *Handbook of floating-point arithmetic*. Springer, 2018.
- 22 A. Ng. Clustering with the  $k$ -means algorithm. *Machine Learning*, 2012.
- 23 X. Pennec. Barycentric subspace analysis on manifolds. *The Annals of Statistics*, 46(6A):2711–2746, 2018.
- 24 F. Preparata and M. Shamos. *Computational geometry: an introduction*. Springer Science and Business Media, 1985.

- 25 Maxim V Shapovalov and Roland L Dunbrack Jr. A smoothed backbone-dependent rotamer library for proteins derived from adaptive kernel density estimates and regressions. *Structure*, 19(6):844–858, 2011.
- 26 D. Ting, G. Wang, M. Shapovalov, R. Mitra, M.I. Jordan, and R. Dunbrack. Neighbor-dependent ramachandran probability distributions of amino acids developed from a hierarchical dirichlet process model. *PLoS Comput Biol*, 6(4):e1000763, 2010.
- 27 C. Yap and T. Dubé. The exact computation paradigm. In *Computing in Euclidean Geometry*, pages 452–492. World Scientific, 1995.
- 28 J. Yu, C. Yap, Z. Du, S. Pion, and Hervé H. Brönnimann. The design of core 2: A library for exact numeric computation in geometry and algebra. In *International Congress on Mathematical Software*, pages 121–141. Springer, 2010.

## A Supporting information

### A.1 Algorithm



■ **Figure 7** An interval where  $F_p$  has an algebraic expression and  $F_p'(\theta) = 0$ . Illustration of  $F_p, F_p', F_p''$  for  $p = 2$  and three angles  $\Theta_0 = \{\theta_1 = 1, \theta_2 = 2, \theta_3 = 3\}$ . Color conventions as in Fig. 1. In this case,  $F_2'(\theta_2) = 0$ , which must be numerically ascertained to ensure the correctness of the algorithm.

■ **Algorithm 2** `Update_root(Sign)`: Updates the `Root_remains` buffer in main algorithm(Algo. 1).

- 
- 1:  $Sign \in \{\text{positive, negative, null}\}$  // Sign of the derivative used to update the presence of roots on  $(\alpha_j, \alpha_{j+1})$
  - 2: `Root_remains`  $\leftarrow$  true // flag indicating whether a root must be sought on  $(\alpha_j, \alpha_{j+1})$
  - 3: **if**  $Sign$  is negative **then**
  - 4:     `Root_remains`  $\leftarrow$  true
  - 5: **else if**  $Sign$  is positive **then**
  - 6:     `Root_remains`  $\leftarrow$  false
  - 7: **else if**  $Sign$  is null **then**
  - 8:     `Root_remains`  $\leftarrow$  false
-

## 15:16 Fréchet Mean

■ **Algorithm 3** `Find_root`( $\alpha_{i-1}, \alpha_i$ ): generic algorithm for  $p > 5$ .

---

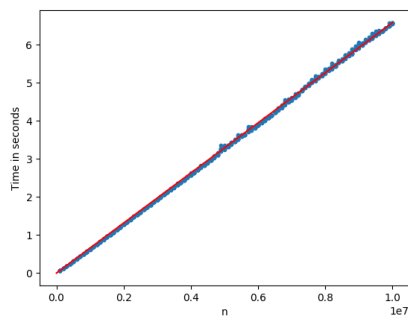
```

1:  $\alpha_{i-1}, \alpha_i$ : the left and right endpoints of the initial interval
2:  $\tau$ : Threshold to stop binary search if interval is small enough
3:  $c$ : Center of interval  $g$ 
4:  $\theta_l \leftarrow \alpha_{i-1}, \theta_r \leftarrow \alpha_i$  // Interval being bisected
5: while Interval_too_wide( $\theta_l, \theta_r$ ) do
6:    $c \leftarrow \theta_l + (\theta_r - \theta_l)/2$ 
7:    $S \leftarrow \text{Sign}(F'_p(c))$ 
8:   if  $S$  is positive then
9:      $\theta_r \leftarrow c$ 
10:  else if  $S$  is negative then
11:     $\theta_l \leftarrow c$ 
12:  else if  $S$  is null then
13:     $\theta_r \leftarrow c$ 
14:     $\theta_l \leftarrow c$ 
15:  $\theta_c \leftarrow \theta_l + (\theta_r - \theta_l)/2$ 

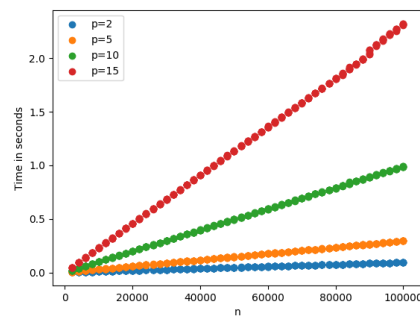
```

---

## A.2 Results



$p = 2, nmax = 10e^7$



$p \in \{2, 5, 10, 15\}, nmax = 10e^5$

■ **Figure 8** Fréchet mean: computation time depending as a function of  $n$  and  $p$ . The samples of size  $n$  are generated at random angles at random in  $[0, 2\pi)$ . **(Left)** The red line joins 0, 0 to the average time of the largest point sets ( $nmax = 10e^7$ ). **(Right)** Each color corresponds to a value of  $p \in \{2, 5, 10, 15\}$ .